

# Reanalysis of Skylab S-194 L-band data in view of validating sea surface roughness corrections for salinity measurements from space

Nicolas Reul, Joseph Tenerelli  
and Bertrand Chapron  
IFREMER

Laboratoire d'Océanographie Spatiale  
Brest, France 29200  
Email: nreul@ifremer.fr

Doug Vandemark  
NASA/GSFC  
Wallops Island, USA

**Abstract**—Of the satellite radiometer sensors, there has been only one instrument that provides any heritage at L-band: the Skylab S-194 instrument that operated in the 1970s. From an analysis of S-194 brightness temperature (Tb) sensitivity to SSS, SST and wind speed, [1] concluded that the wind speed dependence of L-band brightness temperature at nadir is about 0.16 K/knot. This is almost four times higher than what is predicted by recently developed sea surface emissivity models at L-band and twice the experimental value reported during the Bering Sea Experiments [2].

To investigate the possible reasons for such discrepancies, two data sets acquired by the S-194 Skylab instrument from 1973-1974 missions are used in the present paper in conjunction with products from climate model reanalysis projects as ancillary data. The re-analysis shows that it is very likely that [1] overpredicted the quasi-linear wind speed dependence of L-band sea surface emissivity at nadir by a factor of about 2. Main discrepancies being due to different wind speed data used in the analysis. Still, we found that emissivity models for the foam free sea surface based on the small perturbation method underestimate the roughness impact at nadir by a factor of 2. Including the foam impact cannot explain all the differences.

## I. INTRODUCTION

Space-borne sea surface salinity (SSS) observations are considered as a promising technique for future oceanographic satellite missions. New developments in L-band radiometry will provide the key technology to obtain salinity estimates with sufficient accuracy. The ESA SMOS mission, currently under preparation, and the proposed US/Argentinean Aquarius mission will facilitate the first space-borne salinity measurements from 2007 onwards.

The current empirical understanding of the sea surface emissivity at 1.4 GHz mainly relies on a few experiments conducted in the 1970s ([1], [3], [4], [2]) and from recent field studies performed in the context of the future SMOS ([5], [6], [7]) and AQUARIUS ([8]) missions.

Data acquired during these experiments from either towers, aircraft and satellite sensors have all demonstrated that the sea surface emissivity at L-band being dependent on salinity is also function of the ocean surface roughness. Recently conducted

experiments provided estimates of the wind speed sensitivity of L-band sea surface emissivity only for incidence angles larger than 25°. As SMOS will provide multi-angle brightness temperature, it is important to validate roughness corrections for low incidences around nadir as well.

Of the past measurements, there have been only two campaigns that provide near nadir data at L-band: the data from the Skylab spaceborne S-194 radiometer [1] and the Bering sea Experiment aircraft data [2]. From an analysis of S-194 brightness temperature (Tb) sensitivity to SSS, SST and wind speed, [1] concluded that the wind speed dependence of L-band brightness temperature at nadir is about 0.16 K/knot. This is almost four times higher than what is predicted by recently developed sea surface emissivity models at L-band (two-scale [7], and Small Slope Approximation [9]) and twice the experimental value reported by [2] (0.154 K/[m.s<sup>-1</sup>]).

To investigate the possible reasons for such discrepancies, two data sets acquired by the S-194 Skylab instrument from 1973-1974 missions are used in the present paper for re-analysis: (i) the first includes parts of the data set from [10], recently reanalyzed by [11] for Soil Moisture purposes, for which several tracks were available over the ocean, but no coincident ground truth is available; (ii) the second set of data is extracted from the NRL report of [1]. In this analysis, Lerner and Hollinger used an approximate model for the sea water dielectric constant [12] and crude auxiliary data. Using a more accurate dielectric constant model at L-band [13] and products from global model reanalysis (ERA40, WOA01) as auxiliary data, we investigated why the up-to-date emissivity models do not fit the only satellite observations available for validation. In this context, we applied atmospheric and galactic corrections to both Skylab antenna temperature data sets and removed the estimated flat sea surface contribution to estimated surface brightness temperatures. Residuals analysis of the emissivity indicates a sensitivity with wind speed much closer to the Bering sea measurements [2]. Still, the Small Slope Approximation emissivity theory is found to underestimate roughness impact at L-band and nadir.

# Report Documentation Page

*Form Approved*  
*OMB No. 0704-0188*

Public reporting burden for the collection of information is estimated to average 1 hour per response, including the time for reviewing instructions, searching existing data sources, gathering and maintaining the data needed, and completing and reviewing the collection of information. Send comments regarding this burden estimate or any other aspect of this collection of information, including suggestions for reducing this burden, to Washington Headquarters Services, Directorate for Information Operations and Reports, 1215 Jefferson Davis Highway, Suite 1204, Arlington VA 22202-4302. Respondents should be aware that notwithstanding any other provision of law, no person shall be subject to a penalty for failing to comply with a collection of information if it does not display a currently valid OMB control number.

1. REPORT DATE <b>25 JUL 2005</b>	2. REPORT TYPE <b>N/A</b>	3. DATES COVERED <b>-</b>	
4. TITLE AND SUBTITLE <b>Reanalysis of Skylab S-194 L-band data in view of validating sea surface roughness corrections for salinity measurements from space</b>		5a. CONTRACT NUMBER	
		5b. GRANT NUMBER	
		5c. PROGRAM ELEMENT NUMBER	
6. AUTHOR(S)		5d. PROJECT NUMBER	
		5e. TASK NUMBER	
		5f. WORK UNIT NUMBER	
7. PERFORMING ORGANIZATION NAME(S) AND ADDRESS(ES) <b>IFREMER Laboratoire d'océanographie Spatiale Brest, France 29200</b>		8. PERFORMING ORGANIZATION REPORT NUMBER	
9. SPONSORING/MONITORING AGENCY NAME(S) AND ADDRESS(ES)		10. SPONSOR/MONITOR'S ACRONYM(S)	
		11. SPONSOR/MONITOR'S REPORT NUMBER(S)	
12. DISTRIBUTION/AVAILABILITY STATEMENT <b>Approved for public release, distribution unlimited</b>			
13. SUPPLEMENTARY NOTES <b>See also ADM001850, 2005 IEEE International Geoscience and Remote Sensing Symposium Proceedings (25th) (IGARSS 2005) Held in Seoul, Korea on 25-29 July 2005.</b>			
14. ABSTRACT			
15. SUBJECT TERMS			
16. SECURITY CLASSIFICATION OF:			17. LIMITATION OF ABSTRACT
a. REPORT <b>unclassified</b>	b. ABSTRACT <b>unclassified</b>	c. THIS PAGE <b>unclassified</b>	<b>UU</b>
			18. NUMBER OF PAGES <b>4</b>
			19a. NAME OF RESPONSIBLE PERSON

## II. SKYLAB DATA SET RE-ANALYSIS

### A. SkyLab data sets

Skylab was launched on May 14th, 1973 in a near-circular Earth orbit. Orbital inclination was  $50^\circ$  and the nominal altitude was 435 km. The S-194 microwave sensor was a nadir viewing L-band H polarization radiometer. It utilized a fixed planar array antenna oriented toward nadir, recording thermal radiation at a frequency of 1.4 GHz (21-cm wavelength) and measuring the absolute antenna temperature. The sensor used a calibration scheme referenced to fixed hot and cold load input. [1] analyzed several aspects of the data quality of the S-194 sensor, which included an evaluation of the absolute accuracy and stability. Over the course of the entire series of data collection passes (7 through 98) they found that the standard error was approximately 1.3 K with close to zero bias. Half-power beam width of the sensor was  $15^\circ$ , which provided a swath width or resolution footprint of approximately 110 km at an orbital altitude of 435 km. Data were recorded approximately three times per second, which resulted in a distance between centers of two consecutive resolution cells on the ground of 2.5 km.

There were several Earth remote sensing experiments conducted using the S-194 instrument. These included coverage of specific targets and also larger regions that were not the focus of the specific experiment.

[1] state that they had data from 27 passes for their ocean studies. A compendium of all the S-194 measurements analyzed by [1] including collected ground truth data (sea surface temperature (SST), sea surface salinity (SSS), wind speed and sun elevation angle) is available in [1]. The measured antenna temperatures were averaged for a period of several minutes and re-calibrated. Note also that the corresponding estimated ground truth SSS, SST and wind speed data in [1] were given to the nearest 0.5 psu,  $1^\circ\text{C}$  and 1 m/s, respectively.

Other sets of SkyLab S-194 data were recently recovered and reprocessed by [11] to conduct soil moisture analysis (data available on the web). The only data they were able to obtain were those used by [10] corresponding to several days in 1973 and 1974. Portions of several tracks from these data extend over the ocean and are used here for re-analysis. Unlike the analyzed data in [1], the antenna temperature provided by [11] are not averaged but given at about 0.3 Hz, not re-calibrated and as well, no ground truth data are given over the ocean. Figure 1 summarizes the tracks of the S-194 oceanic data available combining these two sources.

### B. Re-analysis

The sea surface brightness temperatures observed by a radiometer at frequency  $f$ , looking at nadir can be expressed as follows:

$$T_B = T_s \cdot \epsilon_s = T_s \left( \left[ 1 - |R^{(0)}|^2 \right] + \Delta e \right) \quad (1)$$

where  $T_s$  is the SST,  $\epsilon_s$  is the sea surface emissivity,  $R^{(0)}$  is the Fresnel reflection coefficient at nadir, and the  $\Delta e$  term is the emissivity changes due to the rough sea surface.

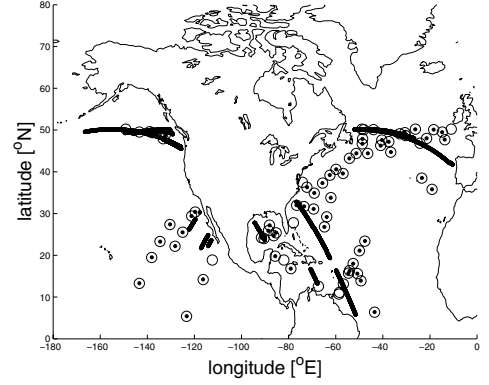


Fig. 1. Locations of available S-194 satellite observations over the ocean. Observations shown are further than 120 km from land. Also, for these observations, sun angles are less than  $70^\circ$

In the following analysis we compare the S-194 satellite-derived emissivity  $\epsilon_s$  with emissivity computed assuming a flat sea surface using the Klein and Swift dielectric constant model [13] applied to SSS and SST data extracted from World Ocean Atlas 2001 (WOA) monthly SSS climatology at  $1^\circ \times 1^\circ$  resolution and ECMWF ERA-40 reanalysis on a  $2.5 \times 2.5^\circ$  grid, respectively. For each satellite measurement we bilinearly interpolate the SSS field nearest in time to the observation point, and we use the same method for SST and 10 m wind.

To derive the sea surface emissivity from the satellite measurements, we must correct the antenna temperatures for atmospheric emission, attenuation, cosmic and galactic radiation, and sun glint. For this analysis we only consider data for which the sun elevation angle is less than  $70^\circ$  and we make no sun glint correction to the remaining data. In this case, we can write the antenna temperature  $T_A$  as

$$T_A = (1 - A)\epsilon_s T_s + T_u + (1 - A)(1 - \epsilon_s) [T_d + T_{gal} + T_{cos}], \quad (2)$$

where,  $A$  is the total atmospheric attenuation from the surface to the satellite,  $\epsilon_s$  is the sea surface emissivity,  $T$  is the SST and  $T_d$ ,  $T_{gal}$ ,  $T_{cos}$   $T_{gal}$  are brightness temperatures corresponding to, respectively, downwelling atmospheric radiation, downwelling galactic radiation, and downwelling cosmic background radiation.

We compute atmospheric attenuation and emission using the Millimeter-wave Propagation Model MPM described in [14]. We consider absorption due to water vapor and molecular oxygen, which are the major contributors to atmospheric absorption and emission at L-band. Although cloud liquid water and ice contribute to atmospheric absorption, their contributions are small relative to those of oxygen and water vapor [15].

For water vapor, temperature and pressure as a function of height, we use ECMWF ERA-40 reanalysis on a  $2.5 \times 2.5^\circ$  grid, which provides data up to about 50 km. For each satellite observation, we use the reanalysis grid nearest in time and then interpolate pressure, temperature and relative humidity in space to the satellite subpoint. We then discretize the atmosphere along the nadir path between the satellite and the

surface into 50 m grid intervals from the surface to 50 km. We then fit natural splines to the model data and compute, at each level, atmospheric absorption coefficients for water vapor and oxygen. If we let  $\alpha(z)$  represent the total absorption coefficient in nepers, then the optical path  $\tau$  between heights  $z_0$  and  $z_1$  is

$$\tau(z_0, z_1) = \int_{z_0}^{z_1} \alpha(z) dz, \quad (3)$$

and the total atmospheric attenuation from  $z_0$  to  $z_1$  is then

$$A(z_0, z_1) = e^{-\tau(z_0, z_1)} \quad (4)$$

The downward atmospheric emission at the sea surface is

$$T_d = \int_{z_s}^{z_t} \alpha(z) T_a(z) A(z_s, z) dz \quad (5)$$

and the atmospheric emission at the top of the atmosphere is

$$T_u = \int_{z_s}^{z_t} \alpha(z) T_a(z) A(z, z_t) dz, \quad (6)$$

In the above expressions for  $T_d$  and  $T_u$ ,  $T_a(z)$  is the atmospheric temperature at height  $z$ ,  $z_s$  is the sea surface height, and  $z_t$  is the top of the atmosphere which is taken to be 50 km.

The cosmic background brightness temperature  $T_{cos}$  is assumed to be 2.7 K and is independent of incidence angle.

For the galactic background brightness temperature  $T_{gal}$  we use the data from [16] and presented in [17]. For simplicity we only consider the contribution from the nadir direction. Using equations presented in [17] we transform each satellite observation location onto the celestial sphere, obtain the galactic brightness contribution, and then attenuate the resulting brightness temperature by the atmosphere to obtain the galactic contribution to  $T_b$  incident at the earth's surface.

### III. RESULTS

Antenna temperatures for all satellite observations are shown in Figure 2. We only considered observations at distances from coast exceeding than 120 km to avoid side-lobe contamination by land. In accordance with [1] and [10], we found atmospheric transmittance and upward atmospheric brightness temperatures of order 0.99 and 2 K, respectively. As illustrated in Figure 3, the total atmospheric and galactic corrections are almost uniform over the complete data set and of order 7-8 K.

Figure 4 shows the difference  $\Delta e$  as function of wind speed between emissivity inferred from S-194 antenna temperatures (corrected for atmospheric, cosmic, and galactic contributions) and emissivity computed by assuming a flat sea surface using the dielectric model of [13] for sea water. Note that in producing this figure, we remove the mean  $\Delta e$  for each pass of the Eagleman and Lin [10] data and for all the Lerner and Hollinger data. This was done to remove clear biases in certain passes (particularly during the month of June) possibly due to calibration issues. The linear best fit through the wind speed-binned averaged data is shown in Figure 4 and exhibits a slope

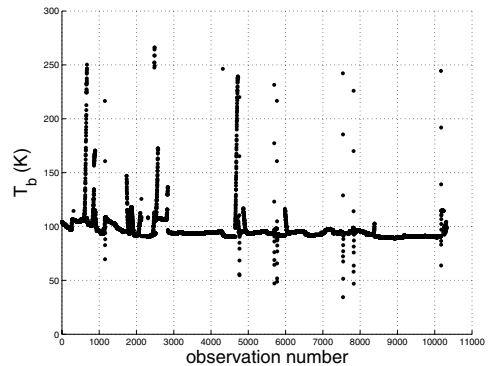


Fig. 2. Antenna temperatures for all satellite observations. These data are not filtered by distance from land and sun angle.

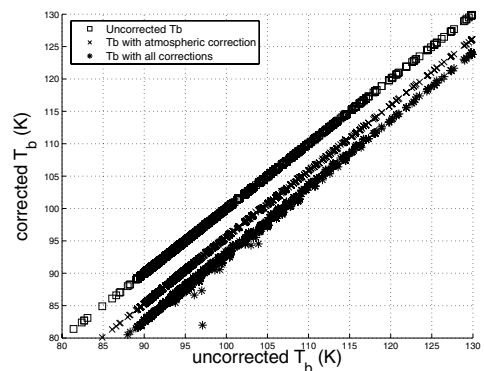


Fig. 3. Scatterplot of corrected and uncorrected brightness temperatures versus uncorrected brightness temperature. Squares show uncorrected brightness temperature; crosses show brightness temperatures corrected for atmospheric attenuation and emission; stars show brightness temperatures corrected for both atmospheric attenuation/emission, cosmic, and galactic radiation at L-band.

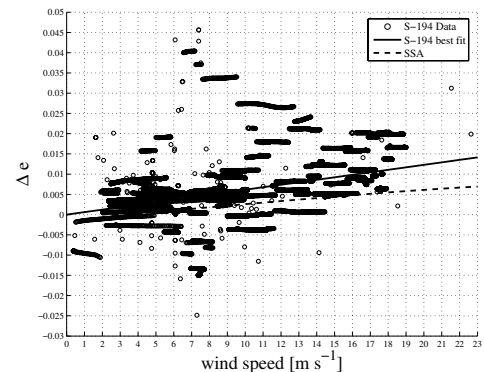


Fig. 4. Difference between emissivities inferred from S-194 antenna temperatures (corrected for atmospheric, cosmic, and galactic contributions) and emissivities computed by assuming a flat sea surface using the dielectric model of [13] for sea water.

of  $6.2 \cdot 10^{-4}$  per  $\text{m.s}^{-1}$  which corresponds approximately to an increase in brightness temperature of about 0.17 K per  $\text{m.s}^{-1}$  at an SST of  $15^\circ\text{C}$ . Assuming an SST of  $0^\circ\text{C}$ , the Bering sea measurements [2] indicates a sensitivity with wind speed of  $5.7 \cdot 10^{-4}$  per  $\text{m.s}^{-1}$ , which is very close from Skylab data deduced sensitivity.

In comparison, we plot as well the results predicted by the Small Slope Approximation (SSA) theory as applied in [9], which exhibits a linear slope of around  $3.5 \cdot 10^{-4}$  per  $\text{m.s}^{-1}$ . Despite the large scatter in the Skylab data, it is clear that SSA model underpredicts the observed wind sensitivity at L-band and nadir.

#### IV. DISCUSSION AND CONCLUSIONS

In preparing for future L-band passive microwave sea surface salinity satellite missions, investigators have employed ground, aircraft and satellite sensors. Of the satellite sensors, there has been only one instrument that provides any heritage at L-band: the Skylab S-194 instrument that operated in the 1970s. Here several dataset from the S-194 missions have been re-analysed expecting that the effort will expand our knowledge of the L-band brightness temperature over the ocean. In this investigation we explored the use of products from climate model reanalysis projects as ancillary or alternative validation data.

Despite a large scatter in the data, which might be due to several reasons (calibration issues, bad quality ancillary data, etc...) the re-analyses showed that it is very likely that [1] overpredicted the quasi-linear wind speed dependence of L-band sea surface emissivity at nadir by a factor of about 2. The results from our reanalysis is consistent with previous aircraft measurements by [2]. As revealed by Figure 5, which shows the linear fits of the wind excess emissivity  $\Delta\epsilon$  for four combinations of auxiliary data, the wind speed data used by Lerner and Hollinger in their analysis are mostly responsible for the different sensitivity observed. Still, we found that emissivity models for the foam free sea surface based on the small perturbation method underestimate the roughness impact at nadir. According to [2], a  $0.07\text{K}/\%$  of whitecap coverage should be expected at nadir. This translates into an increase of the total wind excess emissivity slope of about  $4.3 \cdot 10^{-4}$  per  $\text{m.s}^{-1}$ , still underestimating the observations.

#### REFERENCES

- [1] R. M. Lerner and J. P. Hollinger, "Analysis of microwave radiometric measurements from skylab," NRL, Tech. Rep., Apr. 1976, 93 p.
- [2] W. J. Webster, T. T. Wilheit, D. B. Ross, and P. Gloersen, "Spectral characteristics of the microwave emission from a wind-driven covered sea," *J. Geophys. Res.*, vol. 81, no. 18, pp. 3095–3099, 1976.
- [3] J. P. Hollinger, "Passive microwave measurements of sea surface roughness," *IEEE Trans. Geosci. Electron.*, vol. GE-9, no. 3, pp. 165–169, 1971.
- [4] C. T. Swift, "Microwave radiometer measurements of the Cape Cod Cannal," *Radio Sci.*, vol. 9, no. 7, pp. 641–653, 1976.
- [5] A. Camps, J. Font, M. Vall-llossera, C. Gabarro, R. Villarino, L. Enrique, J. Miranda, I. Corbella, N. Duo, F. Torres, S. Blanch, J. Arenas, A. Julia, J. Etcheto, V. Caselles, A. Weill, J. Boutin, S. Contardo, R. Niclos, R. Rivas, S. Reising, P. Wursteisen, M. Berger, and M. Martn-Neira, "The WISE 2000 and 2001 Campaigns in support of the SMOS Mission: Sea surface L-band Brightness Temperature Observations and their

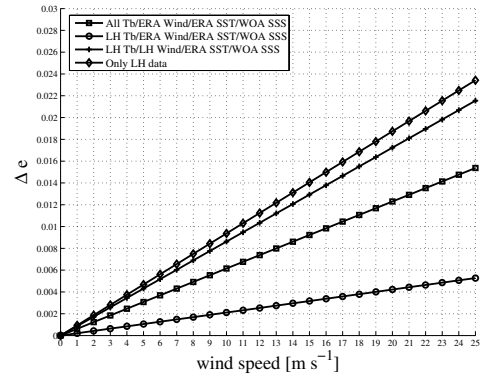


Fig. 5. Linear fits of the wind excess emissivity  $\Delta\epsilon$  for four combinations of data. Squares show the best fit line computed using all brightness temperatures, 10-m wind speed and SST from the ERA40 reanalysis, and SSS from WOA. Circles show the best fit line obtained by using Lerner and Hollinger (LH)  $T_b$ , LH wind and SST data, and WOA SSS. Pluses show the best fit line using LH  $T_b$  data, ERA40 SST and WOA SSS. Diamonds show the best fit line obtained using only data from LH.

- application to Multi-Angular Salinity Retrieval," *IEEE Trans. Geosci. Remote Sensing*, vol. 42, no. 4, pp. 1039–1048, 2004.
- [6] S. Søjbjerg, J. Rotbøll, and N. Skou, "The L-band Ocean Salinity Airborne Campaign, LOSAC," *ESA SP-525*, vol. LOSAC Campaigns Cesbio, pp. pp 27–35, April 2003, p 1743.
- [7] J. Etcheto, E. P. Dinnat, J. Boutin, A. Camps, J. Miller, S. Contardo, J. Wesson, J. Font, and D. Long, "Wind speed effect on L-band brightness temperature inferred from EuroSTARRS and WISE2001 field experiments," *IEEE Trans. Geosci. and Remote Sens.*, vol. 42, no. 10, pp. 2206–2213, 2004.
- [8] W. J. Wilson, S. H. Yueh, J. D. Steven, S. Chazanoff, F. Li, and Y. Rahmat-Samii, "Passive active L- and S-band (pals) microwave sensor for ocean salinity and soil moisture measurements," *IEEE Trans. Geosci. and Remote Sens.*, vol. 39, pp. 1039–1048, 2001.
- [9] N. Reul and B. Chapron, "A simple algorithm for sea surface salinity retrieval from L-Band radiometric measurements at nadir," in *Proceedings of the International Geoscience and Remote Sensing Symposium, IGARSS*, Toulouse, 2003.
- [10] J. R. Eagleman and W. C. Lin, "Remote sensing of soil moisture by a 21-cm passive radiometer," *J. Geophys. Res.*, vol. 81, no. 21, pp. 3660–3666, July 1976.
- [11] H. A. V. d. G. A. Jackson, T.J. and J. R. Eagleman, "Skylab 1 band microwave radiometer observations of soil moisture revisited," *Int. J. Remote Sensing*, vol. 25, pp. 2585–2606, 2004.
- [12] W. W. Ho and W. F. Hall, "Measurements of the dielectric properties of seawater and nacl solutions at 2.65 ghz," *Journal of Geophysical Research*, vol. 78, no. 27, pp. 6301–6315, 1973.
- [13] L. A. Klein and C. T. Swift, "An Improved model of the dielectric constant of sea water at microwave frequencies," *IEEE Trans. Antennas Propag.*, vol. AP-25, pp. 104–111, 1977.
- [14] H. J. Liebe, G. A. Hufford, and M. G. Cotton, "Propagation modeling of moist air and suspended water/ice particles at frequencies below 1000 ghz," in *AGARD 52nd Specialists Meeting of the Electromagnetic Wave Propagation Panel*, Palma de Mallorca, Spain, 1993, pp. 3–1–3–10.
- [15] S. H. Yueh, R. West, W. J. Wilson, F. K. Li, E. G. Njoku, and Y. Rahmat-Samii, "Error sources and feasibility for microwave remote sensing of ocean salinity," *IEEE Trans. Geosci. Remote Sensing*, vol. 39, no. 5, pp. 1049–1060, May 2001.
- [16] P. Reich, J. C. Testori, and W. Reich, "A radio continuum survey of the northern sky at 1420 mhz, the atlas of contour maps," *Astron. Astrophys.*, vol. 376, pp. 861–877, July 2001.
- [17] D. M. LeVine and S. Abraham, "Galactic noise and passive microwave remote sensing from space at L-band," *IEEE Trans. Geosci. Remote Sensing*, vol. 42, no. 1, pp. 119–129, Jan. 2004.